Synthesis of zinc oxide based nanophosphors by solution-combustion method

Vinod Kumar, H. C. Swart and O. M. Ntwaeaborwa
Department of Physics, University of the Free State,
Bloemfontein, ZA9300, South Africa
Email- vinod.phy@gmail.com, swarthc@ufs.ac.za
Tel. +27-514012926

Abstract.
Undoped and doped ZnO nanophosphors (NPr) were synthesized by solution-combustion method. Hexagonal wurtzite structures of ZnO were confirmed by the X-rays diffraction patterns. A broad band orange-red emission from 500 to 850 nm was obtained from the ZnO NPr prepared with the nitrate precursor which may be attributed to oxygen related defects. Terbium doped ZnO (ZnO:Tb) NPr has shown red-green coupled emission. The intensity of the luminescence decreased at higher concentration of Tb due to the formation of Tb_2O_3.

1. Introduction

The optical properties of ZnO studied using photoluminescence (PL), photoconductivity and absorption, reflect the intrinsic direct bandgap, a strongly bound exciton state and gap states due to the point defects [1, 2]. The PL spectra show ultra violet (UV) near band edge emission around 380 nm and defect related deep level emission (DLE), which depends upon the preparation methods and growth conditions. The visible emission is a result of DLE bands present in ZnO [3, 4]. It is important to understand the origin of these emissions for the development of highly efficient optoelectronic devices. A large number of studies on the luminescence properties of ZnO have been investigated and suggested that, the green and red emissions originated from oxygen vacancies (V_o) and zinc interstitials (Zn_i) [5–7]. Other authors have attributed the green emission to both V_o and zinc vacancies (V_{Zn}) [8, 9]. The violet-blue and blue emissions were attributed to Zn_i and V_{Zn}, respectively, in the DLE [10, 11]. The origin of the red emission peaks are attributed to deep level defects such as vacancies and oxygen interstitials, usually observed in the oxygen rich system [12, 13]. Rare-earth (RE) ions like Tb^{3+} are very attractive luminescent centers owing to the high color purity and luminescence efficiency [13].

In this paper, undoped and Tb doped ZnO nano-phosphors (NPr) were synthesized. The PL of undoped and Tb doped are studied and discussed.

2. Experimental details

ZnO NPr were synthesized using the combustion method. Both Zinc acetate dehydrate (ZA) and zinc nitrate tetra hydrates (ZN) were used as precursors, respectively. Zinc precursors and urea were mixed and dissolved in distilled water. A homogeneous solution was obtained after stirring for 20 min. The solution was transferred to a preheated muffle furnace maintained at a temperature of 450°C. All the liquid evaporated and a large amount of heat released resulted in a flame that decomposed there agents further and released more gases. The flame lasted for 60 s and the combustion process was completed within 5 min. These NPr were cooled down to room temperature and were ground gently using a pestle and mortar. Terbium nitrate pentahydrate was used as a dopant source for terbium (Tb). Dopant is used with varying doping concentration from 0.0 to 6.0 mol%.

The crystalline structure of the phosphor was analyzed using a Bruker D8 Advanced powder diffractometer. For chemical states and surface examination, X-ray photoelectron spectroscopy (XPS) using a PHI 5000 Versa probe equipped with monochromatic Al-K_α radiation (hν=1253.6 eV) was conducted. The photoluminescence data was recorded using a He-Cd laser excitation wavelength of 325 nm. The reflectance spectra were collected using a Perkin Elmer Lambda 950 UV-Vis spectrophotometer.

3. Results and discussion

XRD patterns of both the ZN and ZA ZnO NPr are shown in Figure 1. The intensity of the XRD peaks shows that the NPr are highly crystalline. The strong diffraction peaks at 31.71, 34.31 and 36.21° correspond to the (100), (002) and (101) planes of the hexagonal wurtzite structure of ZnO. The preferred orientation corresponding to the plane (101) is the most prominent peak [14].

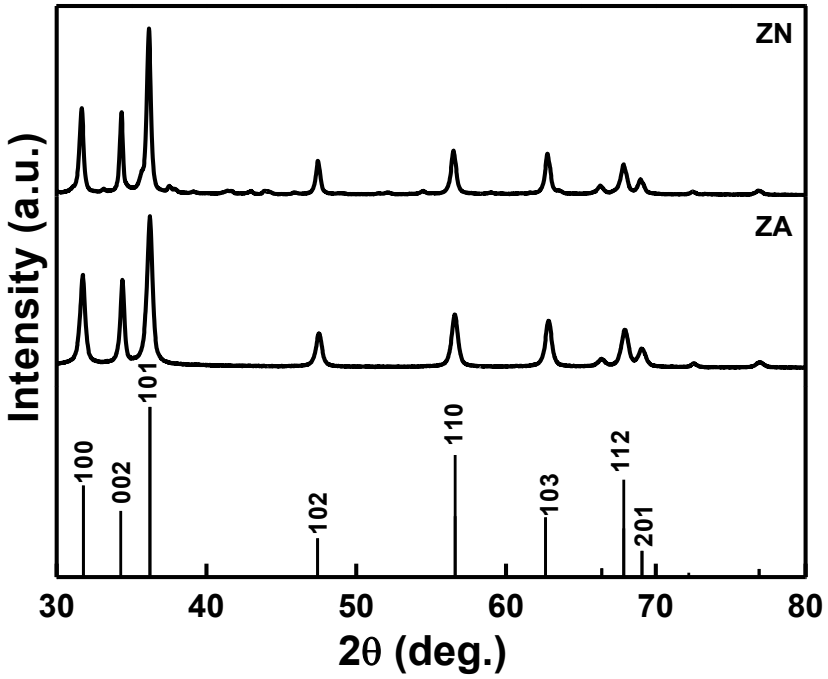

Figure1. XRD spectra of ZnO NPr.

Figure 2(a) displays the optical reflectance spectra of both the ZnO NPr. The ZA sample has less optical reflectance with respect to the ZN sample. It's due to a higher concentration of the defects (V_o) in the sample and provided luminescence killers. The optical bandgap of ZnO NPr is estimated by the extrapolation of the linear portion of the $(\alpha h\nu)^2$ versus $h\nu$ plots. The bandgap is calculated by Tauc's plot method [15]

$$(\alpha h\nu)^2 = A(h\nu - E_g) \tag{4}$$

Where, A is a constant, E_g is optical bandgap, h is plank constant and α is the absorption coefficient. The plot of $(\alpha h\nu)^2$ versus hν for different ZnO NPr is shown in Figure2(b). The bandgap of ZnO NPr was observed at 3.16 eV for both sample.

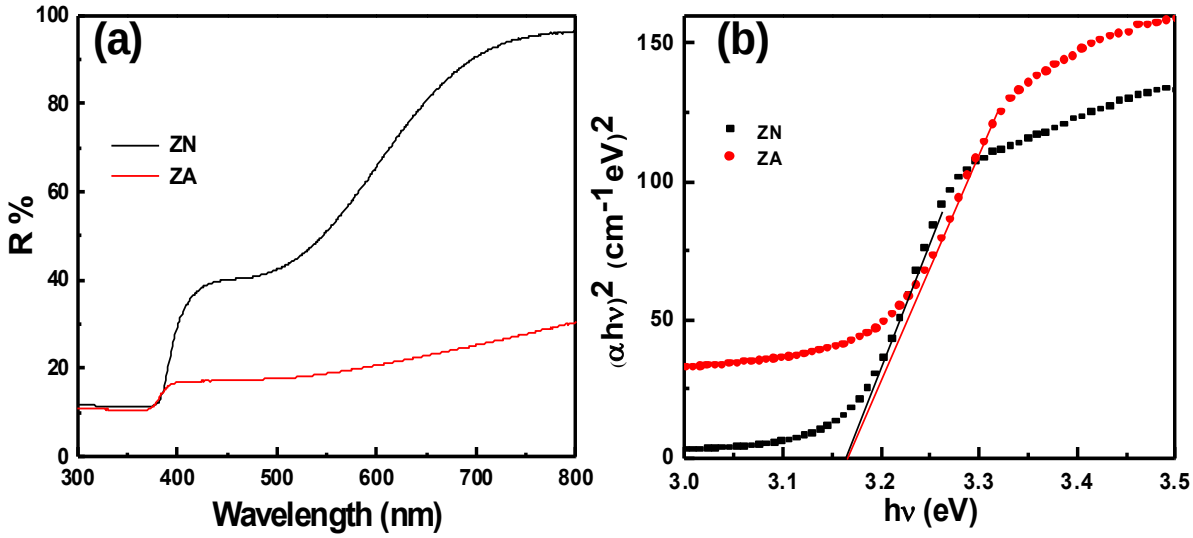

Figure 2. (a) Reflectance curve of ZnO NPr **(b)** band gap by tauc's plots.

Figure 3(a) and (b) shows the de-convoluted oxygen O 1s peaks. The component on the low binding energy side (O1 peak) on spectrum at 530.3±0.3 eV is attributed to O^{2-} ions on the wurtzite structure of a hexagonal Zn^{2-} ion array, surrounded by Zn atoms with their full complement of nearest neighbour O^{2-} ions [16]. In other words, the intensity of this component is a measure of the number of oxygen atoms in a fully oxidised stoichiometric surrounding. The medium binding energy (O2 peak) component centred at 531.2±0.3 eV is associated with O^{2-} ions that are in oxygen deficient regions with in the matrix of ZnO [17, 18] and/or Zn-OH groups [18, 19]. Therefore, changes in the intensity of this component may be partly connected to the variation in the concentration of oxygen defects (V_o or/and oxygen interstitial (Oi)). The higher binding energy (O3 peak) at 532.6±0.3 eV is usually attributed to chemisorbed species (such as CO_3, adsorbed H_2O or O_2) on the surface of the ZnO [18]. The intensity of the O3 peak has decreased after sputtered cleaning due to the removal of surface contaminants. After sputtering, the relative intensity of the O2 peak is much higher for the ZN with respect to the ZA sample, meaning that the concentration of oxygen defect is higher in the case of the ZN. Figure3(c) shows the XPS spectrum of Zn 2p. It contained a doublet, whose binding energies were at 1021.3 and 1044.4 eV, indicating that the Zn atoms were in the Zn 2p oxidation state.

Emission behaviour of ZnO NPr is shown in Figure 3(d). The main features of PL spectra of ZnO can be divided into two categories: near band edge emission and DLE. For the ZA sample, the emission band is composed of a strong UV band around 378 nm, an orange band around 614 nm and a red band around 753 nm. The UV emission band must be explained by a near band-edge transition, namely the free exciton recombination through an excition-excition collision process [20]. An orange-red band had also been observed and it is attributed to defects (O_i and V_o) in ZnO [21-23]. For the ZN sample, the UV band around 392 nm is very weak compared to the orange-red emission. The relative area of the XPS peaks compared to the PL fitted peaks suggests that the orange-red emission intensity and wavelength is definitely affected by the related defects.

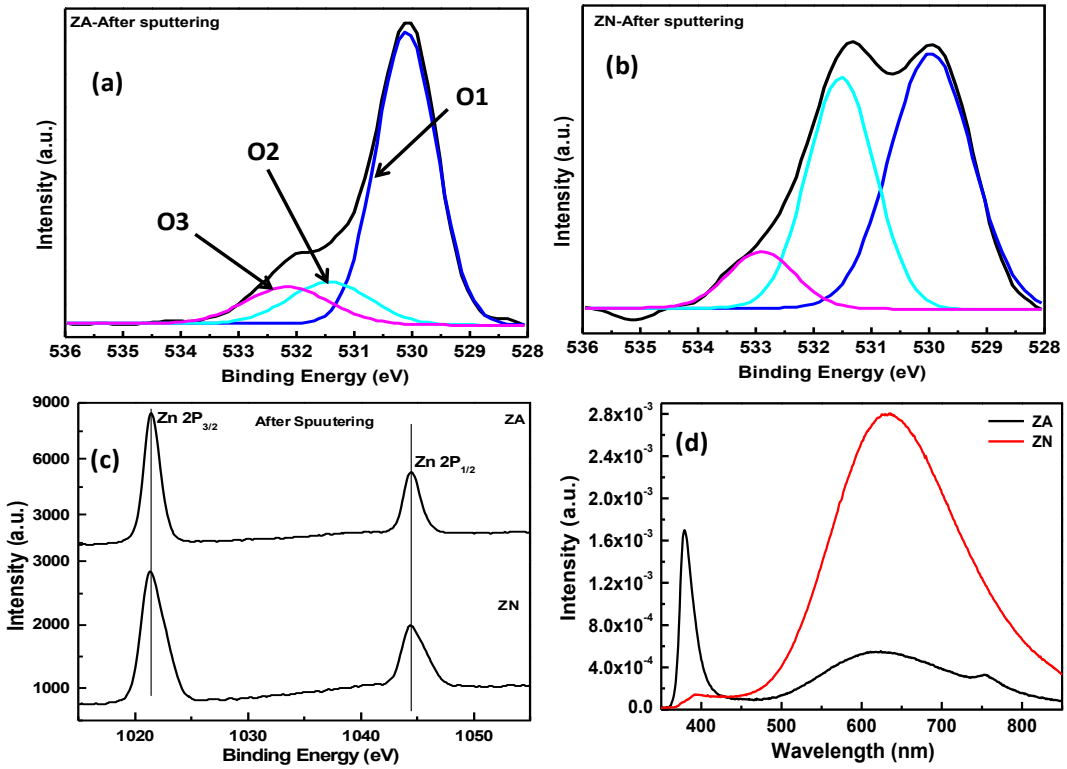

Figure 3. (a) XPS of ZA sample **(b)** XPS of ZN sample **(c)** XPS of Zn peaks **(d)** PL spectra of ZA and ZN.

The XRD spectra of ZnO:Tb with different Tb concentration is shown in Figure 4(a). The strong diffraction peaks at 31.71, 34.31 and 36.21° correspond to the (100), (002) and (101) planes of the hexagonal wurtzite structure of ZnO. At higher doping concentration some other peak is shown. It is due to the formation of Tb_2O_3.

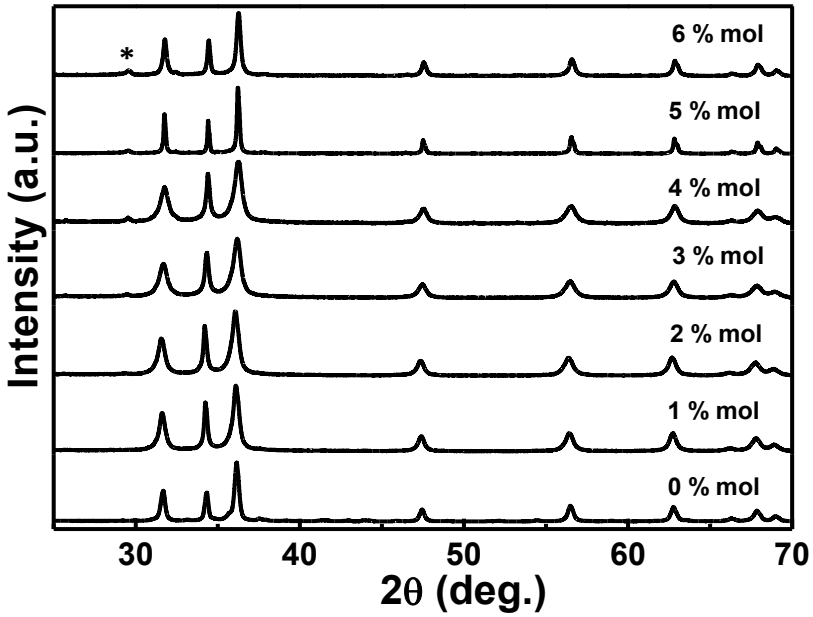

Figure 4. XRD curve of ZnO:Tb with different doping concentration of Tb.

XPS data of oxygen O1s peak ZnO:Tb is shown in Figure 5. In Figure 5 (a), the component on the O1, O2 and O3 peaks on the spectrum is attributed to the contributions discussed above. T higher doping concentration (6 mol%), Tb2O3 peak is also observed. It is attributed to the formation of terbium oxide.

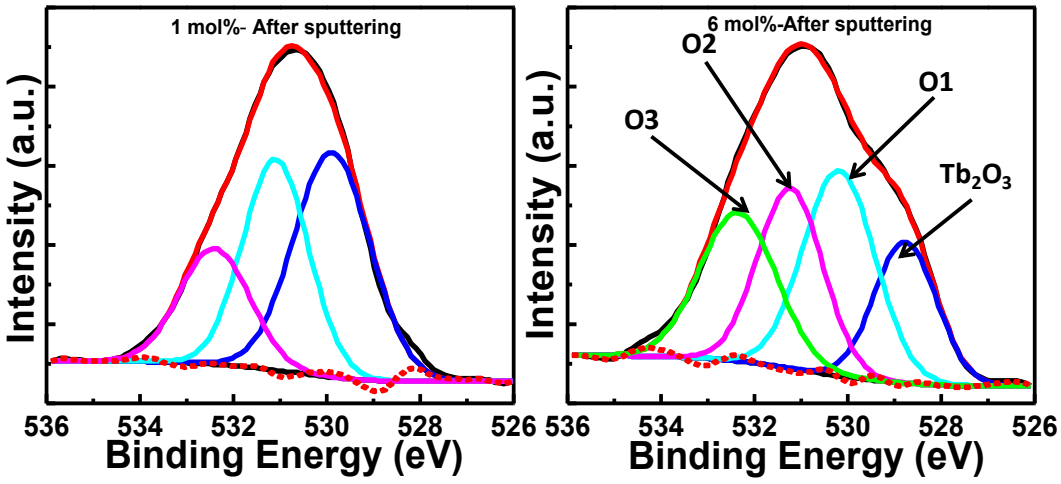

Figure 5. XPS of oxygen peak of ZnO:Tb after 30 sec of Ar sputtering for 1 and 6 mol% Tb.

Figure 6 (a) and (b) shows the PL spectra of ZnO:Tb with different doping concentration of Tb from 0 to 6 mol%. ZnO:Tb shows a green-red coupled emission of the ZN sample. The process of the energy transfer from the ZnO host to Tb through defect states may be described as follows. Firstly, a large amount of electrons are excited from the valence band to the conduction band of the ZnO host. Then non-radiative transition between the conduction band and the surface defects occurs, so the excited electrons may be trapped in the defects and the excitation energy of the ZnO host can be temporarily stored in the defect centers. Because of the short life span of these excited electrons, the energy rapidly transfers from the defects to the dopant ions, and then the higher excited states relax to the main emitting level, so the characteristic emission peaks of dopant ions are observed. As the electrons relax to the defect states of ZnO and recombine with the holes in the valence band, a broad luminescence was observed. The intensity of the $^5D_4$-$^7F_5$ peak has increased with the doping concentration up to 5 mol% of Tb after that it's decreased due to the formation of Tb_2O_3.

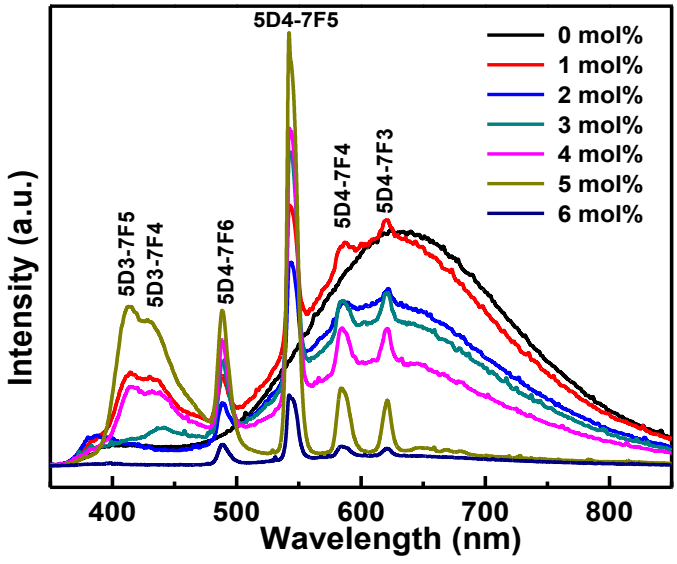

Figure 6. PL spectra of ZnO:Tb with different doping concentration of Tb.

4. Conclusion

Highly crystalline undoped and doped ZnO NPr were synthesized using the solution combustion method. The observed broad PL emission from 500-850 nm is attributed to a coupled emission of orange-red from ZnO. The red emission in ZnO NPr was observed due to the oxygen rich system. Zinc nitrate has shown a good red emission with respect to the zinc acetate based NPr. Orange-red coupled emission is observed in ZnO NPr due to the interstitial and vacancies of oxygen as confirmed by XPS O 1S data. ZnO;Tb NPr has shown green-red coupled emission.

Acknowledgments

This work is based on the research supported by the South African Research Chairs Initiative of the Department of Science and Technology and National Research Foundation of South Africa. The financial support from the Cluster program of the University of the Free State is highly recognised

References

[1] Gutowski J, Presser N, Broser I 1988 *Phys Rev B* **38**, 9746.
[2] Bethke S, Pan H, Wessels BW 1988 *Appl Phys Lett* **52,** 138.
[3] Gong Y, Andelman T, Neumark G, O'Brien S, Kuskovsky I 2007 *Nanoscale Res Lett* **2,** 297
[4] Look DC 2001 *Mater Sci Eng B* **80**, 383.
[5] Yang LL, Zhao QX, Willander M, Yang JH, Ivanov I 2009 *J Appl Phys* **105,** 053503.
[6] Djurisic AB, Leung YH, Tam KH, Hsu YF, Ding L, Ge WK, et al. 2007 *Nanotechnology* **18**,095702
[7] Djurisic AB, Leung YH, Tam KH, Ding L, Ge WK, Chen HY, et al. 2006 *Appl Phys Lett* **88**, 103107
[8] Zhao QX, Klason P, Willander M, Zhong HM, Lu W, Yang JH 2005 *Appl Phys Lett* **87,** 211912
[9] Yamauchi S, Goto Y, Hariu T 2004 *J Cryst Grow* **260,** 1
[10] Cao B, Cai W, Zeng H 2006 *Appl Phys Lett* **88,**161101
[11] Zeng H, Li Z, Cai W, Liu P 2007 *J Appl Phys* **102**, 104307.
[12] Wu L, Wu Y, Pan X, Kong F 2006 *Opt Mater* **28**, 418.
[13] Kumar Vinod, Swart HC, Ntwaeaborwa OM, Kroon RE, Terblans JJ, Shaat SKK, Yousif A Duvenhage MM 2013 *Materials Letters* **101**, 57.
[13] Devi SKL, Sudarsana Kumar K, Balakrishnan A. 2011 *Materials Letters* **65,** 35.
[14] Singh N, Mehra R. M., Kapoor Avinashi, Soga T 2012 *J. Renewable Sustain Energy* **4,** 013110.
[15] Kumar V, Singh RG, Singh F, Purohit LP 2012 *J. Alloys & Comp.* **544** 120.
[16] Chen M, Wang X, Yu YH, Pei ZL, Bai XD, Sun C 2000 *Appl Surf Sci* **158**, 134.
[17] Al-Gaashani R, Radiman S, Daud AR, Tabet N, Al-Douri Y 2013 *Ceram Int* **39**, 2283.
[18] Islam MN, Ghosh TB, Chopra KL, Acharya HN 1996 *Thin Solid Films* **280**, 20.
[19] Kim YS, Tai WP, Shu SJ 2005 *Thin Solid Films* **491,** 153.
[20] Ahn CH, Kim YY, Kim DC, Mohanta SK, Choa HK 2009 *J. Appl. Phys.* **105**, 013502.
[21] Kong YC, Yu DP, Zhang B, Fang W, Feng SQ 2007 *Appl Phys Lett* **78,** 407.
[22] Pierce BJ, Hengehold RL 1976 *J Appl Phys* **47,** 644.
[23] Studenikinm SA, Golegu N, Cocivera M 1998 *J Appl Phys* **84,** 2287.